Pharmaceutical Research, Vol. 22, No. 1, January 2005 (© 2005)
DOI: 10.1007/s11095-004-9017-z

Research Paper

Antibodies as Drug Carriers III: Design of Oligonucleotides with Enhanced Binding Affinity for Immunoglobulin G

Enzo Palma,[1] David G. Klapper,[2] and M. J. Cho[1,3]

Received May 24, 2004; accepted September 14, 2004

Purpose. To understand the structural requirements in designing epitope-bearing oligonucleotides with high antibody-binding affinity.
Methods. Binding affinity (K_A) and stoichiometry (n) of dinitrophenyl (DNP)-derivatized model 27-mer oligonucleotides (ODNs), $GGG(AAA)_7GGG$, to monoclonal anti-trinitrophenyl (TNP) antibodies were determined using isothermal titration calorimetry (ITC). Structural variations were made in the ODNs to assess the effects of antigenic valence, epitope density, inter-epitope linker length, and linker flexibility. Binding isotherms were fitted with a single binding-site model to obtain K_A and n, from which changes in Gibbs free energy ($\Delta G°$), entropy ($\Delta S°$), and enthalpy ($\Delta H°$) were derived.
Results. As expected, ligands displaying increased epitope density showed increases in K_A: for example, K_A for $(DNP)_2$-Cys is 3.3-fold greater than that for DNP-Lys. Introduction of multiple DNP groups via long and flexible linkers to one end of the 27-mer ODN resulted in a bivalent behavior with n value of 1. A bivalent ligand, derivatized at both ends with a long and flexible linker, failed to form an immune complex when hybridized to its antisense strand, presumably due to intercalation of the DNP moiety to the double strand. ODNs derivatized with flexible linkers exhibited a higher K_A than those with a rigid linker. Ligands with flexible inter-epitope linkers measuring distances of 110, 60, and 40 Å yielded 13-, 30-, and 13-fold increases in K_A, respectively. The combination of these factors; namely, bivalence, flexible inter-epitope linkers, and optimal inter-epitope distance, resulted in an overall 66-fold increase in K_A. Thermodynamic analysis of binding indicates that the formation of high-affinity ODN-IgG complexes was a spontaneous and exothermic event, characterized by large negative $\Delta S°$, $\Delta H°$, and $\Delta G°$ values.
Conclusions. All four strategies tested during this investigation, namely bivalence, epitope density, inter-epitope linker flexibility, and optimal inter-epitope distance, proved to be useful in improving the binding affinity of DNP-labeled ODNs to anti-TNP IgG. The final ODN design incorporating these strategies will be used in testing the systemic pharmacokinetic advantage gained from complexing such ODNs to IgG.

KEY WORDS: antibodies as systemic drug carriers; binding affinity (K_A); isothermal titration calorimetry (ITC); oligonucleotide (ODN); thermodynamics.

INTRODUCTION

Antisense and immune-modulating synthetic oligonucleotides (ODNs) have emerged as new therapeutic agents targeted to a variety of malignancies, including cancer (1,2). Their clinical potential is very promising; however, once systemically administered, these compounds face various transport and metabolic barriers that compromise their delivery to target tissues. For example, oligonucleotides invariably suffer from poor systemic pharmacokinetics (mainly short half-life and nucleolytic degradation), which prevent them from fully exerting their therapeutic effect (3,4). In light of these challenges, this laboratory has been exploring the possibility of using endogenous antibodies as systemic drug carriers for prolonging the systemic $t_{1/2}$ of ODNs and preventing systemic nucleolytic degradation (5). With this approach, we exploit the finding that monomeric immune complexes (i.e., complexes in a 1:1 or 2:1 ligand-to-antibody ratio) can effectively lengthen the apparent $t_{1/2}$ of the complexed drug molecule to that of the antibody itself; for example, 21 days for human IgG_1 (6,7).

In our previous studies, mice immunized against fluorescein showed at least a 100-fold decrease in the initial disappearance rate of fluorescein derivatives of a small model drug molecule (6) as well as of a model protein of MW 22 kDa (7). Here, the anti-fluorescein antibodies serve as high affinity

[1] Division of Drug Delivery and Disposition, School of Pharmacy, The University of North Carolina, Chapel Hill, North Carolina 27599, USA.
[2] Department of Microbiology and Immunology, The University of North Carolina, Chapel Hill, North Carolina 27599, USA.
[3] To whom correspondence should be addressed. (e-mail: m_j_cho@unc.edu)

ABBREVIATIONS: DNP, dinitrophenyl; DNP-6C, dinitrophenyl-aminohexane linker; DNP-TEG, dinitrophenyl-tetraethyleneglycol linker; Fab, antigen binding site on IgG; IC, immune complex; IgG, immunoglobulin G; ITC, isothermal titration calorimetry; K_A, equilibrium association constant or binding affinity; MW, molecular weight; ODN, oligonucleotide; SDS-PAGE, sodium-dodecyl sulfate polyacrylamide gel electrophoresis; TNP, trinitrophenyl.

($K_A > 10^7$ m^{-1}) and low capacity drug carriers (two binding sites per IgG molecule of MW 150 kDa) (8). As expected, the pharmacokinetics of these model drug molecules expressing a single epitope fluorescein critically depended on antibody titer as well as antigen-binding affinity (6,7). However, at a given level of titer, which would be the case for endogenous antibodies, the overall pharmacokinetic behavior of these immune complexes will predominantly depend on the intrinsic antibody binding affinity constant, K_A. As such, our approach is distinct from the common use of monoclonal antibodies as drug targeting ligands. It is instead similar to employing long circulating serum proteins, such as albumin, as drug carriers.

Antibody binding naturally occurs with multivalent antigens that effect the formation of large polymeric, precipitable immune complexes that rapidly clear from the systemic circulation (9–11). To avoid this event and attain sustained systemic circulation, two requirements must be met. First and foremost, the epitope should be introduced to the ODN in such a way that the antigen-antibody interaction is in a monomeric fashion (i.e., in a 1:1 or 2:1 ligand-to-antibody ratio). Second, the binding affinity as expressed by K_A must be high so that premature ligand dissociation does not occur while in the systemic circulation (6).

In an effort to optimize binding affinity, a series of model 2,4-dinitrophenyl (DNP)-derivatized ODNs were designed with variations in three major factors involved in binding to anti-2,4,6-trinitrophenyl (TNP)-monoclonal IgG_1 ($mIgG_1$): epitope valence, flexibility of linker between DNP and ODN, and inter-epitope distance. Because IgG is a flexible, bivalent protein, with a distance between its antigen-binding sites (F_{ab}) ranging from 4 to 12 nm (12,13), model ODNs were designed to reflect these conditions and tested for their propensity to complex anti-TNP IgG_1 using isothermal titration calorimetry (ITC). Binding affinity (K_A), complex stoichiometry (n), and subsequently thermodynamic parameters such as changes in enthalpy (ΔH°), entropy (ΔS°), and Gibbs free energy (ΔG°) were derived. Pharmacokinetic analysis of these immune complexes will be the subject of future studies.

MATERIALS AND METHODS

Preparation and Characterization of Anti-TNP $mIgG_1$ Antibodies

Monoclonal anti-trinitrophenyl (TNP) IgG_1 was produced by the UNC Lineberger Cancer Center using hybridoma cell line 1B7.11 (ATCC no. TIB-191). The harvested culture medium was dialyzed extensively (SpectraPor, MW cutoff 100 kDa) against phosphate buffered saline (PBS, pH 7.0) and further purified via protein-G affinity column chromatography (Amersham Pharmacia, Piscataway, NJ, USA). Antibody purity was confirmed via SDS-PAGE after extensive dialysis against 10mM, pH 8.0 Tris buffer (single band, results not shown). Stock antibody concentrations were estimated using the BCA assay (Biorad, Hercules, CA, USA).

Preparation and Characterization of DNP-Labeled Oligonucleotides

Model oligonucleotides (sense, 5′-GGG$(AAA)_7$GGG-3′; antisense, 5′-CCC$(TTT)_7$CCC-3′) were synthesized and labeled with DNP (sense strands only) by Oligos Etc (Wilsonville, OR, USA) and Oswel, Inc. (Southampton, UK) using phosphoramidite solid-phase chemistry. ODNs were purified via reverse-phase DMT-on HPLC and PAGE and supplied at a purity of >90%. Two types of DNP labels were used: DNP-TEG (Glen Research, Sterling, VA, USA) provides a flexible, ethylene glycol-based, 18-atom DNP-label that can be introduced multiple times during synthesis, whereas DNP-6C (Oswel) is a rigid alkyl DNP label that places the DNP epitope only 6 carbons away from the DNA backbone (Fig. 1). Moreover, SPACER 9, a 12 Å tri(ethylene glycol) spacer-phosphoramidite derivative (Glen Research) was introduced between successive DNP-TEG linkers during solid phase synthesis (Oligos Etc) to lengthen inter-epitope distance (Fig. 1). For the most part, DNP-labeling occurred at the 5′-oligonucleotide terminal and it was reasonably assumed that due to the bilateral symmetry displayed by these oligomers (Table I) that derivatization at the 3′ terminal would have yielded a similar DNP-derivative with regard to anti-DNP antibody binding. Monovalent controls, namely DNP-Lys and $(DNP)_2$-Cys, were purchased from Sigma (St. Louis, MO, USA).

Sense and antisense strands were dissolved in 1.0 ml of 10 mM Tris buffer at pH 8.0 containing 50 mM NaCl and 1 mM EDTA (TE buffer) and stock concentrations estimated spectrophotometrically [ε_{260}: 3.15×10^5 $m^{-1}cm^{-1}$ (sense) and ε_{260}: 2.13×10^5 $m^{-1}cm^{-1}$ (antisense), estimated using nearest neighbor analysis] (14). Duplexes were formulated by mixing equimolar concentrations of sense and antisense ODNs, heating to 90–95°C in a heatblock, and cooling to room temperature on the benchtop. Proper hybridization was confirmed via nucleic acid PAGE (Biorad). Single stranded antigens were used as supplied by the manufacturers, without further processing; see Table I.

Isothermal Titration Calorimetry and Thermodynamic Analysis

Titration was performed at the UNC Macromolecular Interactions Facility using a VP-ITC microcalorimeter (Mi-

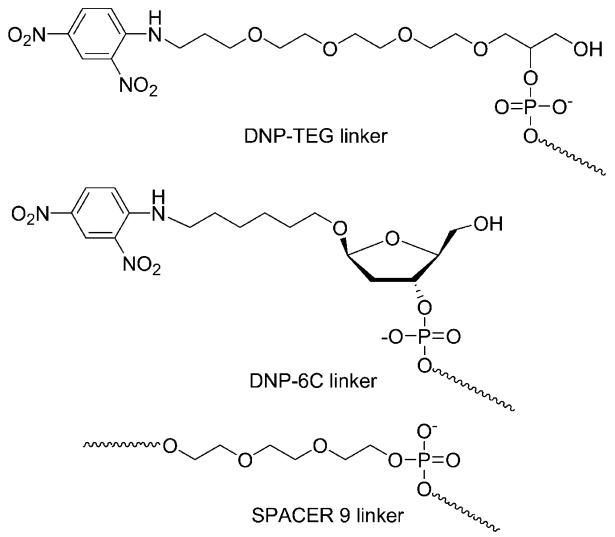

Fig. 1. DNP-derivatization reagents. DNP-TEG is a flexible poly-(ethylene glycol)-based linker approximately 22.5 Å in length; DNP-6C is a rigid six-carbon alkyl DNP linker approximately 10 Å in length; SPACER 9 is a flexible tri(ethylene glycol)-based spacer incorporated between two DNP-TEG linkers. Its length is approximately 12 Å.

Table I. Structure of DNP-Ligands and Their Binding Parameters to Monoclonal Mouse Anti-TNP IgG_1[a]

Structure (conformation)[b]	Inter-epitope distance (Å)[c]	K_A (M^{-1})[d]	n[e,i]	ΔH° (kcal mol^{-1})[f]	ΔS° (cal mol^{-1} K^{-1})	ΔG° (kcal mol^{-1})
Monovalent ligands						
I. Nε-2,4-DNP-D-lysine	N/A[h]	3.9×10^6	2.0	–11.2	–7.5	–8.9
II. N,S-di(2,4-DNP)-L-cysteine	N/A	1.3×10^7	1.8	–4.6	17.0	–9.7
III. DNP-TEG-$G_3(A_3)_7G_3$ (f)	N/A	6.5×10^6	1.8	–8.8	1.6	–9.3
Bivalent ligands						
IV. DNP-TEG-$G_3(A_3)_7G_3$-TEG-DNP (f)	137	1.5×10^7	1.0	–14.1	–14.8	–9.7
V. DNP-6C-$G_3(A_3)_7G_3$-6C-DNP (f)	111	1.9×10^8	0.8	–33.9	–75.7	–11.3
VI. DNP-6C-$G_3(A_3)_7G_3$-6C-DNP (r) $C_3(T_3)_7C_3$	111	2.6×10^7	0.8	–33.0	–76.4	–10.2
VII. DNP-TEG-SPACER 9--$G_3(A_3)_7G_3$ (f) DNP-TEG--|	60	4.3×10^8	0.9	–63.3	–172.9	–11.8
VIII.[g] (DNP-TEG)$_3$-$G_3(A_3)_7G_3$ (f)	48	1.9×10^8	1.1	–31.4	–67.3	–11.3
IX.[g] (DNP-TEG)$_3$-$G_3(A_3)_7G_3$ (f) $C_3(T_3)_7C_3$	48	1.3×10^8	1.1	–29.2	–60.5	–11.2
Multivalent ligands						
X. (DNP-TEG)$_3$-$G_3(A_3)_7G_3$-(DNP-TEG)$_3$ (f)	137	7.2×10^7	0.6	–65.0	–181.9	–10.8
XI.[g] (DNP-TEG)$_3$-$G_3(A_3)_7G_3$-(DNP-TEG)$_4$ (f) $C_3(T_3)_7C_3$	48	4.7×10^8	0.6	–44.9	–110.9	–11.9

[a] Antigen valence and mode of binding based on ITC binding stoichiometry; sense ODN sequence is in 5′ → 3′ direction.
[b] f: flexible, r: rigid.
[c] Estimated lengths based on 3.4 Å per nucleotide of DNA and a random walk model (Ref. 18); DNP-TEG: ~22.5 Å; SPACER 9: ~12.0 Å; DNP-6C: ~10Å.
[d] % errors in K_A are 2–8%.
[e] % errors in n are 1–5%.
[f] % errors in ΔH° are 1–4%.
[g] Mediate binding across DNP-TEG linkers; see Fig. 3.
[h] N/A: not applicable.
[i] Binding stoichiometry of ligand to antibody.

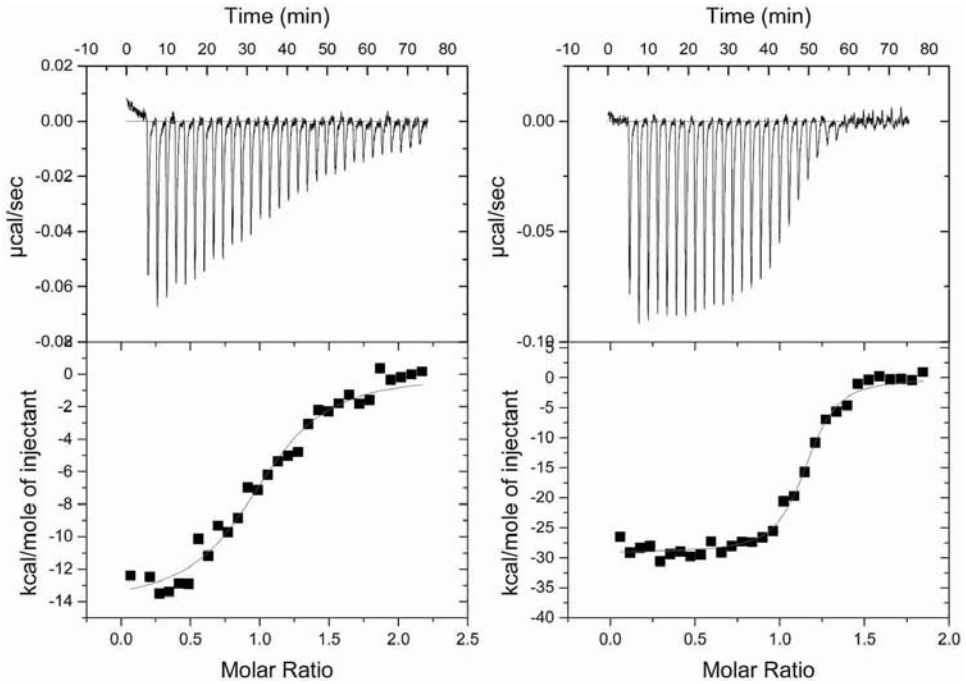

Fig. 2. Calorimetric titration of **IV** (left) and **IX** (right) with anti-TNP IgG in 10 mM Tris buffer at pH 8.0. Briefly, the titrating syringe was filled with the ligand of interest (250 μl, 20 μM in 10 mM Tris buffer at pH 8.0) and titrated onto a sample cell containing anti-TNP $mIgG_1$ (1.5 ml, 1 μM in 10 mM Tris buffer at pH 8.0). A typical analysis would comprise 25–30 5-μl injections, spaced 120 s apart, at 25°C.

crocal, Inc; Northampton, MA, USA). All samples were degassed and cooled to 20°C prior to analysis. Analyte concentrations varied according to the expected stoichiometry of binding. For the most part, a 20-fold excess of ligand was used to compensate for any dilution effects during titration. Briefly, the titrating syringe was filled with the ligand of interest (250 μL, 20 μM) and titrated onto a sample cell containing anti-TNP $mIgG_1$ (1.5 ml, 1 μM). A typical analysis would comprise 25–30 5-μl injections, spaced 120 s apart, at 25°C (Fig. 2). Data analysis and fitting were performed using the ITC analysis software, Origin 5.0 (Microcal, Inc.) All calorimetric data was corrected for heats of dilution prior to curve fitting with a single binding site model. Control experiments were conducted with underivatized ODNs with no discernable calorimetric interaction. Equilibrium association constants (K_A), ligand-to-antibody binding stoichiometry (n), ΔH°, and ΔS° were obtained directly from the ITC output, whereas ΔG° was derived using the following equation:

$$\Delta G^\circ = -RT \ln K_A = \Delta H^\circ - T\Delta S^\circ$$

RESULTS AND DISCUSSION

Monovalent Complexation

As shown in Table I, three monovalent ligands were tested for their ability to complex anti-TNP IgG. This study was carried out primarily to establish a reference point in assessing the effect of ligand valence and epitope density on K_A. As expected, monovalent ligands were complexed in a 2:1 ligand-to-antibody stoichiometric ratio as depicted on Fig. 3, panel A. Complexation occurred with K_A in the range of 10^6~10^7 m^{-1} (Table I). In the case of $(DNP)_2$-Cys (ligand **II**, Table I), a compound displaying two DNP epitopes in close proximity, a complete sequestration of the two closely located DNP-moieties inside the F_{ab} binding pocket was expected, as

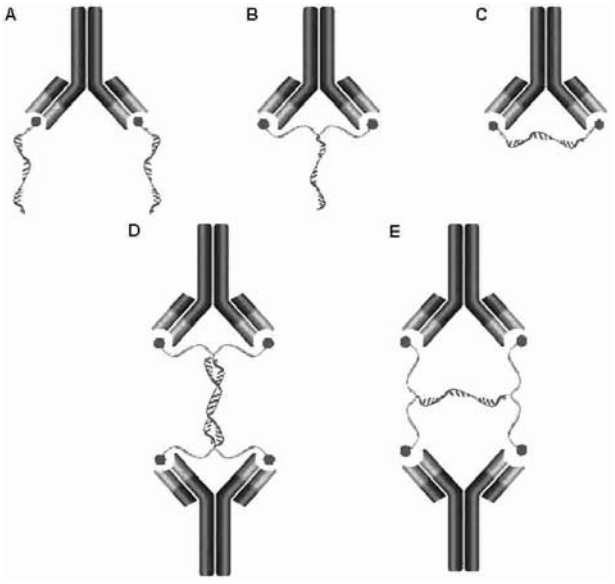

Fig. 3. Binding models for ODN immune complexation based on binding stoichiometry. (A) monovalent complexation (**III**); (B) bivalent complexation (**VII–IX**); (C) bivalent complexation (**IV–VI**); (D) multivalent complexation (**XI**); and (E) multivalent complexation (**X**). The additional third DNP-TEG linker on **VIII–XI** was omitted from panels B, D, and E for clarity purposes.

Table II. Effect of Epitope Density and MW of Monovalent Ligands on K_A

Ligand[a]	n[b]	K_A (M^{-1})	DNP content	MW (Da)	ΔK_A (fold-difference)
I	2.0	3.9×10^6	1	348.7	1.0
II	1.8	1.3×10^7	2	453.3	3.3
III	1.8	6.5×10^6	1	8993.0	1.7

[a] Reference ligand is shaded gray.
[b] Binding stoichiometry of ligand to antibody.

seen with other structurally similar compounds (15,16). Doubling the epitope density of these two small molecules (**I** vs. **II**), where the epitope is significant in size relative to the whole, resulted in a 3.3-fold enhancement of K_A (Table II). Such gain is thought to result from a large decrease in k_{off}, the complex dissociation rate constant, caused by the simultaneous binding of two DNP-epitopes within each F_{ab} (17). A concomitant increase in k_{on}, the association rate constant, is also thought to have occurred since increasing epitope density raises the probability of binding by increasing the local effective concentration of binding epitopes. These two events contribute to a large increase in K_A; hence, epitope clustering represents a feasible strategy to maximize binding affinity.

It is worthy to note that **VIII** and **IX**, which display a clustering of DNP epitopes on the 5′-terminals, were originally intended to test the effect of epitope density on K_A. As such, these ligands were expected to result in high-affinity monovalent binding to anti-TNP IgG with n value of 2. It was thus surprising to observe that they bound anti-TNP IgG in a bivalent fashion with n value of 1 (Table I). We attribute these findings to the length and flexibility of the DNP-TEG linkers present in these ligands (Fig. 1). The inter-epitope distance is estimated to be 48 Å, effectively creating a bivalent environment suitable for binding the antibody in a monomeric fashion (Fig. 3, panel B). Here and throughout this report, the inter-epitope distance was estimated based on extra- and intrapolation of the data on the end-to-end distance of various sizes of poly(ethylene glycol) chains (18). It was also observed that a 26-fold increase in MW (**I** of MW 348.7 vs. **III** of MW 8,993.0) resulted in 1.7-fold enhancement of K_A (Table II). This finding that the increased MW did not have a deleterious effect on complexation was somewhat counterintuitive in terms of so-called binding orientation hypothesis (7).

Bivalent Complexation

Ligand **IV** represents a prototypical bivalent ODN in which the DNP moieties both at the 3′- and 5′-terminals effectively mediate monomeric binding across the DNA backbone (Fig. 3, panel C). However, once hybridized to its complementary ODN, the resulting double stranded ODN failed to bind IgG (data not shown). Due to the length and flexibility of the DNP-TEG linker used to derivatize this ligand, the DNP epitope can loop back and intercalate itself into the ODN backbone. Such a phenomenon has been observed with other structurally related ODN labels (19) and it was, in our case, supported spectrophotometrically (significant suppression of OD_{360}; data not shown). To resolve this problem and confirm our hypothesis on the intercalation of DNP-TEG, ligand **V** was prepared with a much shorter and rigid DNP-ODN linker (DNP-6C, Fig. 1). Such modification

Table III. Effect of Antigenic Valence, Linker Flexibility, and Inter-Epitope Distance on K_A

Dependent variable	ODNs[a]	n[b]	K_A (M^{-1})	Linker flexibility[c]	Inter-epitope distance (Å)[e]	ΔK_A (fold-difference)
Antigenic valence	III	2.0	6.5×10^6	N/A[d]	N/A	1.0
	IV	1.0	1.5×10^7	N/A	N/A	2.3
Linker flexibility	VI	0.8	2.6×10^7	Rigid	N/A	1.0
	V	0.8	1.9×10^8	Flexible	N/A	7.3
Inter-epitope distance	IV	1.0	1.5×10^7	N/A	137	1.0
	V	0.8	1.9×10^8	N/A	111	12.6
	VII	0.9	4.3×10^8	N/A	60	28.7
	VIII	1.1	1.9×10^8	N/A	48	12.7
Combined effect	III	1.8	6.5×10^6	N/A	N/A	1.0
	V	0.8	1.9×10^8	Flexible	111	29.1
	VII	0.9	4.3×10^8	Flexible	60	66.2
	VIII	1.1	1.9×10^8	Flexible	48	29.2

[a] Reference ligand is shaded gray.
[b] Binding stoichiometry of ligand to antibody.
[c] Refers to inter-epitope linker.
[d] N/A: not applicable.
[e] Estimated lengths based on 3.4 Å per nucleotide of DNA and a random walk model (Ref. 18); DNP-TEG: ~22.5 Å; DNP-6C: ~10 Å; SPACER 9: ~12 Å.

proved to be sufficient in preventing DNP-intercalation and expected binding profiles between anti-TNP IgG and ligand **V** and its hybridized analog **VI** were clearly observed (Table II).

As shown on Table III, bivalent binding effectively increased the overall K_A of complexation, relative to monovalent ligand **III**. A 2.3-fold increase in K_A was observed in the case of **IV**, consistent with a 2-fold increase in valence. In contrast, **V** and **VIII** exhibited a 29-fold increase in K_A compared with **III** (Table III). Such a large increase in binding affinity was unexpected, however, it is speculated that these oligonucleotides not only reflect the effect of bivalence but also the effect of inter-epitope distance and linker flexibility (see below). Similarly, **VII** yielded a surprisingly high K_A value (66-fold increase), thought to result from the aforementioned additive effect and not from individual contributions from bivalence.

The rigidity of the linker bridging the two DNP epitopes also had a direct effect on binding affinity. Hybridization of **V** to its complimentary strand, which resulted in a rigid structure **VI** (Table I), had a detrimental effect on binding, manifested by a 7-fold reduction in binding affinity (Table III). These results confirm that linker flexibility is necessary to achieve high affinity binding to IgG, a flexible molecule itself (12,13).

Similarly, the distance between DNP epitopes greatly influenced the magnitude of K_A. Direct comparison of the binding affinities of **IV**, our prototypical bivalent ODN, to that of **V**, **VII**, and **VIII** discerned this effect. Table III displays such relationship: **V** and **VIII** exhibit a 13-fold increase in binding affinity upon reduction of their inter-epitope distance from 137 Å (**IV**) to 111 Å and 48 Å, respectively. Ligand **VII**, which has an inter-epitope distance of 60 Å, displays a 29-fold enhancement in binding affinity.

The high degree of dependence of K_A on antigenic valence, inter-epitope distance, and linker flexibility highlights the importance of considering physical dimensions of the antibody when designing its ligands. Such was the approach taken by Paar *et al.* (20) and Baird *et al.* (18) when testing the F_{ab} cross-linking ability of a series of ligands displaying different degrees of valence, flexibility, and inter-epitope distances. Their results corroborate the dependence of high-affinity antibody binding on inter-epitope distance, antigenic valence, and ligand flexibility. Such are also our findings.

Multivalent Complexation

Ligands **X** and **XI** (Table I) were designed to test the additive effect of bivalence, epitope density, and linker flexibility on binding affinity. These ligands were successively derivatized, on both terminals, with three DNP-TEG linkers and subsequently tested as such (**X**) or hybridized to their complimentary strands (**XI**). Unfortunately, as shown on Table IV, the stoichiometry of binding indicated the formation of dimeric complexes between these ligands and anti-TNP IgG. Nevertheless, such interaction exhibited enhanced binding affinity, thought to result from the increased binding capacity of these ligands. As shown on Table IV, the dimeric binding of **XI** is 6.5-fold higher than **X**. We interpret this observation based on the difference in binding patterns involved: Fig. 3 panel D and E for **XI** and **X**, respectively. Three observations support this analysis: a) the 6.5-fold enhance-

Table IV. Effect of Binding Capacity on K_A During Multivalent Complexation

ODNs[a]	n[b]	K_A (M^{-1})	Hybridization state[c]	Linker flexibility[d]	ΔK_A (fold-difference)
IV	1.0	1.5×10^7	s.s. (flexible)	Flexible	1.0
X	0.6	7.2×10^7	s.s (flexible)	Flexible	4.8
IX	1.1	1.3×10^8	d.s (rigid)	Flexible	1.0
XI	0.6	4.7×10^8	d.s (rigid)	Flexible	3.6
X	0.6	7.2×10^7	s.s (flexible)	Flexible	1.0
XI	0.6	4.7×10^8	d.s (rigid)	Flexible	6.5

[a] Reference ligand is shaded gray.
[b] Binding stoichiometry of ligand to antibody.
[c] s.s: single stranded; d.s.: double stranded.
[d] Refers to inter-epitope linker.

ment of K_A seen with **XI**, the hybridized analogue of **X**, is not characteristic of a rigid ligand but of a flexible compound, as seen with **V** vs. **VI** (Table I); b) a 4.8-fold enhancement in binding affinity was observed when comparing **X** to its structural analogue, **IV** (Table IV). It is assumed that due to their structural similarity (Table I), these ligands bind IgG similarly (i.e., across their DNA backbone), however, an enhancement in binding affinity is observed due to an increase in binding capacity (two vs. one IgG molecules, respectively); and c) similar analysis of binding affinities between structural analogues **XI** and **IX** (Table I), the latter known to bind IgG across its DNP-TEG linkers (Fig. 3, panel B; Table I), reveal a 3.6-fold enhancement in binding affinity (Table IV). This again is attributed to the increased binding capacity of **XI**. Although these ligands display enhanced affinity, utilizing two antibodies for the systemic transport of one oligonucleotide is neither energetically nor cost efficient. As seen in this investigation, monomeric ligands can be structurally tailored to yield high binding affinities when complexing IgG (**VII** vs. **XI**, Table I) without having to implement higher epitope densities or binding capacities.

Thermodynamic Analysis

As shown on Table I, immune complexation is associated with large negative ΔH° and ΔG°, both indicative of exothermic and spontaneous reactions. The observed decreasing trend in ΔS° supports the tighter binding indicated by the increasing trend in K_A, since a negative change in entropy is characterized in the present case by the loss of molecular freedom. Taken together, these thermodynamic parameters suggest that the binding of a bivalent, flexible ODN displaying an optimal inter-epitope distance is an event more thermodynamically favored than that of a ligand partially displaying the aforementioned characteristics.

It is worthy to note that **II**, which displays two DNP epitopes in close proximity, as shown on Table I, caused a positive change in entropy, a trend not seen with other ligands. It is speculated that this positive change is caused by a dramatic displacement of water molecules within the paratope resulting from the accommodation of two epitopes inside the antibody's binding pocket. This event is contrasted to the interaction of one epitope per paratope seen with all the other ligands, which exhibit negative entropic changes (Table I).

CONCLUSIONS

The optimal oligonucleotide design for high-affinity immune complexation resembles that of **VII**. This ODN is a single stranded, flexible ligand terminally displaying two DNP-TEG linkers spaced apart by a 12 Å tri(ethylene glycol) linker, SPACER 9. Its design incorporates three of the four strategies tested during this investigation; that is, bivalence, a flexible inter-epitope linker, and an optimal inter-epitope distance (60 Å). Implementation of such characteristics result in a 66-fold increase in binding affinity over monovalent ligands (Table III). It remains to be seen if the high-affinity binding of an ODN to immunoglobulins, be they naturally occurring endogenous antibodies or from active immunization, can provide a circulatory life long enough for targeted delivery *in vivo*.

ACKNOWLEDGMENTS

This study was supported in part by NIH grant GM 57557 and NRSA pre-doctoral fellowship 5F31 CA099929-02.

REFERENCES

1. A. F. Carpentier, G. Auf, and J.-Y. Delattre. CpG-Oligonucleotides for cancer immunotherapy: review of the literature and potential applications in malignant glioma. *Front. Biosci.* **8**:115–127 (2003).
2. P. Sazani and R. Kole. Therapeutic potential of antisense oligonucleotides as modulators of alternative splicing. *J. Clin. Invest.* **112**:481–486 (2003).
3. S. Agrawal, J. Temsamani, W. Galbraith, and J. Tang. Pharmacokinetics of antisense oligonucleotides. *Clin. Pharmacokinet.* **28**: 7–16 (1995).
4. S. T. Crooke, M. J. Graham, J. E. Zuckerman, D. Brooks, B. S. Conklin, L. L. Cummins, M. J. Greig, C. J. Guinosso, D. Kornbrust, M. Manoharan, H. M. Sasmor, T. Schleich, K. L. Tivel, and R. H. Griffey. Pharmacokinetic properties of several oligonucleotide analogs in mice. *J. Pharmacol. Exp. Ther.* **277**:923–937 (1996).
5. G. Burdick and W. Emlen. Effect of antibody excess on the size, stoichiometry, and DNAse resistance of DNA anti-DNA immune complexes. *J. Immunol.* **135**:2593–2597 (1985).
6. B. N. Rehlaender and M. J. Cho. Anti-drug antibodies as drug carriers. I. For small molecules. *Pharm. Res.* **18**:745-752 (2001).
7. B. N. Rehlaender and M. J. Cho. Antibodies as drug carriers. II. For proteins. *Pharm. Res.* **18**:753–760 (2001).
8. B. N. Rehlaender and M. J. Cho. Antibodies as drug carriers. *Pharm. Res.* **15**:1652–1656 (1998).
9. M. Head, N. Meryhew, and O. Runquist. Mechanism and computer simulation of immune complex formation, opsonization, and clearance. *J. Lab. Clin. Med.* **128**:61–74 (1996).
10. M. Mannik, A. O. Haakenstad, and W. P. Arend. The fate and detection of circulating immune complexes. In L. Brent and J. Holborow (eds.), *Progress in Immunology II*, American Elsevier, New York, 1974, pp. 91–101.
11. T. Skogh, O. Stendahl, T. Sundqvist, and L. Edebo. Physiochemical properties and blood clearance of human serum albumin conjugated to different extents with dinitrophenyl groups. *Int. Arch. Allergy Appl. Immun.* **70**:238–241 (1983).
12. L. J. Harris, E. Skaletsky, and A. McPherson. Crystallographic structure of an intact IgG1 monoclonal antibody. *J. Mol. Biol.* **275**:861–872 (1998).
13. K. H. Roux, L. Strelets, and T. E. Michaelsen. Flexibility of human IgG subclasses. *J. Immunol.* **159**:3372–3382 (1997).
14. J. SantaLucia Jr., H. T. Allawi, and P. A Seneviratne. Improved nearest-neighbor parameters for predicting DNA duplex stability. *Biochemistry* **35**:3555–3562 (1996).
15. A. B. Edmundson, K. R. Ely, X. M. He, and J. N. Herron. Cocrystallization of an immunoglobulin light chain dimer with bis(dinitrophenyl) lysine: tandem binding of two ligands, one with and one without accompanying conformational changes in the protein. *Mol. Immunol.* **26**:207–220 (1989).
16. A. B. Edmundson, J. N. Herron, K. R. Ely, X. M. He, D. L. Harris, and E. W. Voss Jr. Synthetic site-directed ligands. *Philos. Trans. R. Soc. Lond. B Biol. Sci.* **323**:495–509 (1989).
17. S. Kulin, R. Kishore, J. B. Hubbard, and K. Helmerson. Real-time measurement of spontaneous antigen-antibody dissociation. *Biophys. J.* **83**:1965–1973 (2002).
18. E. J. Baird, D. Holowka, G. W. Coates, and B. Baird. Highly effective poly(ethylene glycol) architectures for specific inhibition of immune receptor activation. *Biochemistry* **42**:12739–12748 (2003).
19. J. Telser, K. A. Cruickshank, L. E. Morrison, and T. L. Netzel. Synthesis and characterization of DNA oligomers and duplexes containing covalently attached molecular labels: comparison of biotin, fluorescein, and pyrene labels by thermodynamic and optical spectroscopic measurements. *J. Am. Chem. Soc.* **111**:6966–6976 (1989).
20. J. M. Paar, N. T. Harris, D. Holowka, and B. Baird. Bivalent ligands with rigid double stranded DNA spacers reveal structural constraints on signaling by FcεRI. *J. Immunol.* **169**:856–864 (2002).